

Structural, electronic and magnetic properties of metal–metal bonded dinuclear rhenium complexes bridged by organocyanide acceptor ligands †

Stuart L. Bartley, Mervin J. Bazile, Jr., Rodolphe Clérac,‡ Hanhua Zhao, Xiang Ouyang and Kim R. Dunbar*

Department of Chemistry, Texas A&M University College Station, Texas 77842-3012, USA.

E-mail: dunbar@mail.chem.tamu.edu

Received 24th April 2003, Accepted 22nd May 2003

First published as an Advance Article on the web 12th June 2003

The syntheses, spectroscopic properties, redox chemistry, and solid-state structures of products obtained from the reaction of $\text{Re}_2\text{Cl}_4(\text{dppm})_2$ (dppm = bis(diphenylphosphino) methane) with the polycyano acceptors TCNQ (7,7,8,8-tetracyanoquinodimethanido) and DM-DCNQI (2,5-dimethyl-*N,N'*-dicyanoquinonediimine) are described. The compounds $[\text{Re}_2\text{Cl}_4(\text{dppm})_2](\mu\text{-TCNQ})$, **1**, and $[\text{Re}_2\text{Cl}_4(\text{dppm})_2](\mu\text{-DM-DCNQI})$, **2**, have been prepared by reaction of two equivalents of $\text{Re}_2\text{Cl}_4(\text{dppm})_2$ with TCNQ and DMDCNQI, respectively, in THF or CH_2Cl_2 . A single-crystal X-ray crystallographic study of $[\text{Re}_2\text{Cl}_4(\text{dppm})_2](\mu\text{-TCNQ}) \cdot 10\text{THF}$ revealed the presence of a *trans*- μ_2 bidentate mode for the bridging TCNQ ligand that joins two $\text{Re}_2\text{Cl}_4(\text{dppm})_2$ molecules through equatorial positions. In a similar fashion, the compound $[\text{Re}_2\text{Cl}_4(\text{dppm})_2](\mu\text{-DM-DCNQI}) \cdot 10\text{THF}$ consists of two Re_2 units coordinated to the two nitrile positions of the DM-DCNQI ligand. The electronic properties of both compounds are unusual in that they exhibit intense, broad absorptions that span the near-IR region and extend into the mid-IR. The electrochemistry of the compounds consists of numerous oxidation and reduction processes in the range of +2.0 to –2.0 V as determined by cyclic voltammetry. Both **1** and **2** exhibit temperature independent paramagnetism (TIP) with large χ_{TIP} values of 7.29×10^{-3} and $6.23 \times 10^{-3} \text{ emu mol}^{-1}$, respectively.

Introduction

Research in materials chemistry has witnessed an explosion of activity in recent years, due, in part, to the quest for novel materials that can be used in developing technologies. Although high-temperature solid-state chemistry continues to figure prominently in the materials arena, there is heightened interest in molecule-based materials prepared from low-temperature solution routes. Frontrunners in this field include the organic charge-transfer salt TCNQ-TTF (TCNQ = 7,7,8,8-tetracyanoquinodimethane; TTF = tetrathiafulvalene), the first molecular crystal to exhibit metallic behavior, and the Bechgaard salts $(\text{TMTSF})_2\text{X}$ (TMTSF = tetramethyltetraselenafulvalene) which are among the first organic superconductors.¹ In the area of molecular-based magnetic materials,² notable early examples are soluble ferromagnets prepared from Cp_2^*M (M = Fe, Mn) and polycyano acceptor molecules such as TCNQ and TCNE (tetracyanoethylene).³ In the course of this research, Manriquez and Miller *et al.* discovered that the reaction between $\text{V}(\text{C}_6\text{H}_6)_2$ and TCNE yields a room-temperature magnet formulated as $\text{V}(\text{TCNE})_2 \cdot 0.5\text{CH}_2\text{Cl}_2$ which is believed to contain σ -bound TCNE.⁴ This finding is part of a new direction for transition metal polycyano acceptor chemistry, namely the use of organic acceptors such as TCNQ and TCNE as nitrile ligands in their radical anion forms.

In our research laboratories, we are exploring the chemistry of donor molecules of the type $\text{M}_2\text{X}_4(\text{PR}_3)_4$ and $\text{M}_2\text{X}_4(\text{P-P})_2$ (X = Cl, Br; M = Mo, Re, W; R = Me, Et, Prⁿ; P–P = dppm, dppe) with TCNQ and related organic acceptors such as DM-DCNQI (2,5-dimethyl-*N,N'*-dicyanoquinonediimine). In addition to being coordinatively unsaturated, many of these molecules undergo accessible oxidation processes.⁵ In particular, the triply-bonded dirhenium complex $\text{Re}_2\text{Cl}_4(\text{dppm})_2$ exhibits two

reversible oxidations at $E_{1/2(\text{ox})} = +0.35 \text{ V}$ and $E_{1/2(\text{ox})} = +0.87 \text{ V}$ vs. Ag/AgCl, which renders it well-suited for charge-transfer reactions with TCNQ whose first reduction potential is located at $E_{1/2(\text{red})} = +0.28 \text{ V}$ (Fig. 1).^{5a,6} In addition to being ideally suited to undergo spontaneous redox chemistry with each other, the Re_2 donor and the organocyanide acceptor also possess accessible π symmetry HOMOs which will enhance electronic delocalization between dimetal units that are connected through the bridging organic group. Based on this rationale, we set out to study the charge-transfer reactions of the metal–metal bonded donor complex $\text{Re}_2\text{Cl}_4(\text{dppm})_2$ with TCNQ and DM-DCNQI. Herein we report the X-ray structures of two “dimer-of-dimers” complexes in which two $\text{Re}_2\text{Cl}_4(\text{dppm})_2$ molecules are linked by TCNQ or DM-DCNQI. The spectroscopic and physical properties of these unusual products are described as well.

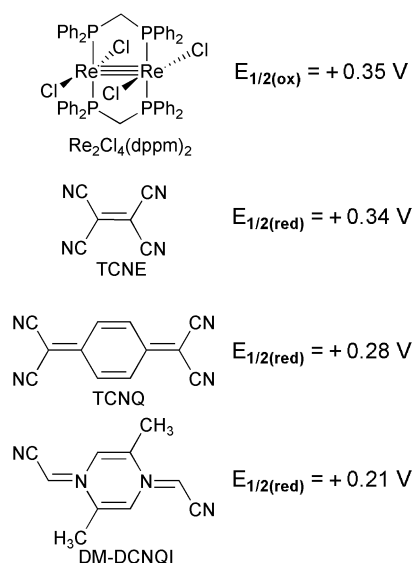


Fig. 1 Selected precursors used for charge-transfer reactions.

† Electronic supplementary information (ESI) available: Fig. S1: Cyclic voltammogram of **1**; Fig. S2: Differential pulse voltammogram of **1**; Fig. S3: Cyclic voltammogram of **2**. See <http://www.rsc.org/suppdata/dt/b3/b304509a/>

‡ Present address: Centre de Recherche Paul Pascal, Avenue du Dr. Schweitzer, 33600 Pessac, France.

Table 1 A comparison of the $\nu(\text{C}\equiv\text{N})$ and $\nu(\text{C}=\text{C})$ stretching frequencies for various TCNQ containing compounds

Compound	$\nu(\text{C}\equiv\text{N})/\text{cm}^{-1}$	$\nu(\text{C}=\text{C})/\text{cm}^{-1}$	Nitrile coordination
TCNQ	2222 (vs)	1542 (s)	None
$[\text{Bu}_4\text{N}][\text{TCNQ}]$	2181 (s), 2156 (m)	1594 (s)	None
LiTCNQ	2200 (s), 2114 (s, br)	1581 (s)	None
1 ^a	2187 (m), 2109 (s, br)	1573 (m)	$\sigma\text{-}\mu^2$
$[\text{FeCp}^*][\text{TCNQ}]$	2179 (s), 2153 (m)	^b	None
$[\text{CrCp}^*][\text{TCNQ}]$	2178 (s), 2153 (m)	^b	None
$[\text{MnCp}^*(\text{CO})_2][\text{TCNQ}]$	2200 (m), 2110 (w)	1585 (m)	σ
$[\text{MnCp}^*(\text{CO})_2]_4[\text{TCNQ}]$	2170 (w), 2105 (s)	^b	$\sigma\text{-}\mu^4$

^a **1** = $[\text{Re}_2\text{Cl}_4(\text{dppm})_2]_2(\mu\text{-TCNQ})$. ^b Not reported.

Results and discussion

The electron-rich complex $\text{Re}_2\text{Cl}_4(\text{dppm})_2$ reacts spontaneously with the acceptor molecules TCNQ and DM-DCNQI to form highly colored solutions and dark brown-black THF-insoluble products. Crystals of the products $[\text{Re}_2\text{Cl}_4(\text{dppm})_2]_2(\mu\text{-TCNQ})\cdot 10\text{THF}$, **1**·10THF, and $[\text{Re}_2\text{Cl}_4(\text{dppm})_2]_2(\mu\text{-DM-DCNQI})\cdot 10\text{THF}$, **2**·10THF, with interstitial THF molecules of crystallization were isolated from a careful layering of separate THF solutions of the two reactants. The structures of both **1**·10THF and **2**·10THF, determined by single-crystal X-ray diffraction methods, revealed the presence of a bridging bidentate mode for both TCNQ and DM-DCNQI.

A. $[\text{Re}_2\text{Cl}_4(\text{dppm})_2]_2(\mu\text{-TCNQ})$, **1**

(i) Synthesis and spectroscopic properties. One equivalent of TCNQ reacts with two equivalents of $\text{Re}_2\text{Cl}_4(\text{dppm})_2$ in THF to yield black microcrystals of **1**. The infrared spectral features of **1** are quite unusual in comparison to typical charge-transfer products of TCNQ. Selected infrared data for **1** are listed along with corresponding data for TCNQ^0 and TCNQ^- in Table 1. From these data, one can conclude that the compound is not an outer-sphere charge-transfer product of TCNQ, but rather a molecule that contains σ -coordinated TCNQ. The determination of the X-ray crystal structure of **1**·10THF provided confirmation for this hypothesis. The infrared spectrum of **1** exhibits stretching modes at 2187 and 2109 cm^{-1} attributed to the $\nu(\text{C}\equiv\text{N})$ of the unbound and bound CN groups of TCNQ respectively. The intense $\nu(\text{C}\equiv\text{N})$ band at 2109 cm^{-1} is assigned to the bound nitrile in **1** and is shifted to a lower frequency as a result of significant $\text{d}_\pi\text{-}\pi^*$ back-bonding. As the $\text{C}\equiv\text{N}$ bond lengthens, the π^* orbitals are stabilized, and as the $\text{C}\equiv\text{N}$ bond becomes longer, the M–N distance decreases, thus increasing the overlap of the $\text{d}_\pi\text{-}\pi^*$ orbitals.⁷ Moreover, it has been shown that metal ions with strong back-bonding interactions to nitriles (a net metal-to-ligand charge transfer) exhibit an intensity enhancement of the $\text{C}\equiv\text{N}$ stretch.⁷ It is also interesting to note that the degree of charge transfer in various TCNQ complexes can be estimated from the nitrile stretching frequencies.⁸ A comparison of the $\text{C}\equiv\text{N}$ and $\text{C}=\text{C}$ stretching frequencies of **1** with TCNQ^0 and TCNQ^- suggests the assignment of a 1– charge to the bridging TCNQ in **1**, which requires each dirhenium moiety to bear a partial formal charge of +0.5.

In addition to the infrared spectra, the electronic absorption spectra (UV-visible, near and mid IR regions) reveal interesting behavior for the product $[\text{Re}_2\text{Cl}_4(\text{dppm})_2]_2(\mu\text{-TCNQ})$. The spectrum of **1** performed in CH_2Cl_2 (Fig. 2) contains intense absorptions at $\lambda_{\text{max}} = 1080$ ($\epsilon = 2.56 \times 10^4 \text{ M}^{-1} \text{ cm}^{-1}$) and 1980 ($\epsilon = 2.20 \times 10^4 \text{ M}^{-1} \text{ cm}^{-1}$) nm. The low energies as well as intensities of these absorptions are quite unusual and are unlike any transitions exhibited by the starting materials. In the case of $\text{Re}_2\text{Cl}_4(\text{dppm})_2$, a weak d–d transition occurs at $\lambda_{\text{max}} = 510$ nm ($\epsilon = 4.70 \times 10^2 \text{ M}^{-1} \text{ cm}^{-1}$) and TCNQ^0 displays a sharp $\pi\rightarrow\pi^*$ transition at 400 nm.

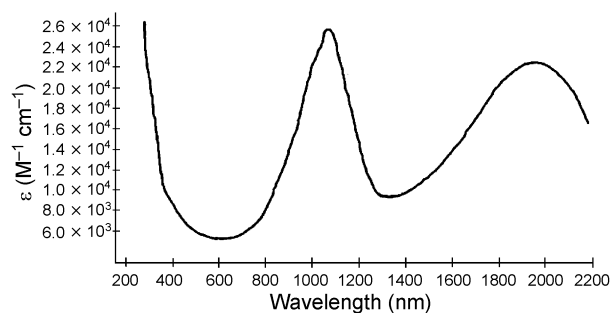


Fig. 2 Electronic absorption spectrum of $[\text{Re}_2\text{Cl}_4(\text{dppm})_2]_2(\mu\text{-TCNQ})$, **1**, in CH_2Cl_2 .

(ii) X-Ray crystal structure of $[\text{Re}_2\text{Cl}_4(\text{dppm})_2]_2(\mu\text{-TCNQ})\cdot 10\text{THF}$, **1·10THF.** The preliminary structure of **1** was reported earlier in a brief communication by our group.⁹ A single-crystal X-ray study of **1**·10THF confirms its 2 : 1 formulation, and reveals the presence of a μ_2 -bridging mode for TCNQ. The molecular structure of **1**·10THF, depicted in Fig. 3, consists of two Re_2 units that are linked through the *trans* cyanide groups of a bridging TCNQ molecule. The molecule is centrosymmetric, with the midpoint of the TCNQ moiety being situated on an inversion center. A packing diagram looking down the *a*-axis is provided in Fig. 4.

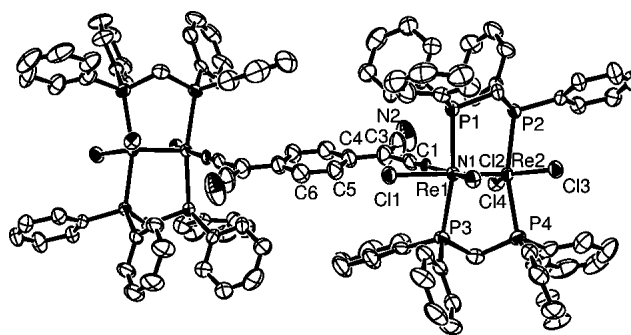


Fig. 3 Thermal ellipsoid representation of $[\text{Re}_2\text{Cl}_4(\text{dppm})_2]_2(\mu\text{-TCNQ})\cdot 10\text{THF}$, **1**·10THF.

During the refinement procedure it became necessary to fix the position of C(1). When allowed to refine unconstrained, the N(1)–C(1) distance became unreasonably short at 0.92 Å, which is considerably less than the distance of 1.03 Å that first appeared in the difference map. Furthermore, the C(1)–C(2) distance lengthens to an unreasonably long distance of 1.52 Å when unconstrained. Models that included fixing N(1) and C(1) were examined. When only N(1) was fixed, the N(1)–C(5) distance became 0.90 Å, and when C(1) was fixed, the N(1)–C(1) distance refined to 1.023(8) Å. The latter refinement was chosen because it is the most chemically reasonable model. In addition to the aforementioned refinements, the identities of the N and C atoms were switched such that the group was treated as an isonitrile, but this led to poorer refinements. The artificially

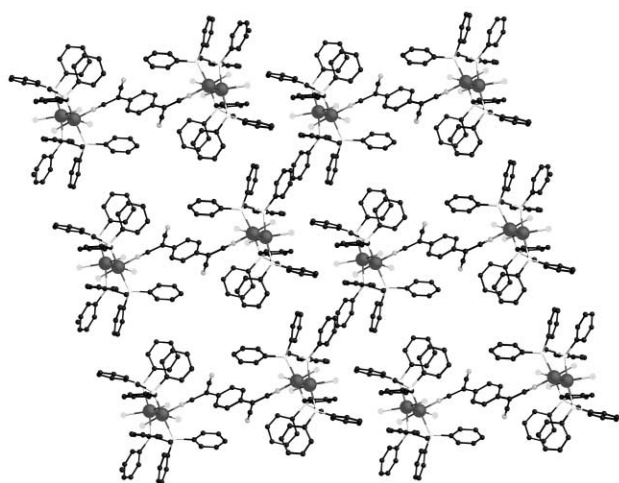


Fig. 4 Packing diagram of $[\text{Re}_2\text{Cl}_4(\text{dppm})_2]_2(\mu\text{-TCNQ})\cdot 10\text{THF}$, viewed down the a axis.

short C–N distance that refines without constraint is attributed to librational disorder of the CN groups which serves to distort the thermal ellipsoids and thus prevents an accurate assignment of the atom locations for bond distance calculations. It should be noted that the unligated C(3)–N(2) moiety refines to a reasonable C–N distance of 1.148(10) Å.

The coordination geometries of the two Re atoms within each M_2L_9 unit are different (see Fig. 5). The nitrile-substituted metal center, Re(1), adopts an octahedral arrangement consisting of an axial chloride, Cl(1), as well as an equatorial chloride Cl(2), and an equatorial nitrogen ligand, N(1) in addition to the *trans* dppm ligands. The geometry around Re(2) is trigonal bipyramidal which is similar to the geometries of the Re atoms in the parent complex $\text{Re}_2\text{Cl}_4(\text{dppm})_2$. Distances and angles are within the usual ranges for derivatives of $\text{Re}_2\text{Cl}_4(\text{dppm})_2$.¹⁰ A list of selected bond distances and angles is provided in Table 2. Of special note is the Re–Re separation of 2.2895(4) Å, which is longer than the distance of 2.234(3) Å found in the parent triply-bonded complex. In the absence of other considerations, one would predict a shorter metal–metal bond resulting from depopulation of an antibonding orbital upon oxidation (*i.e.* $\sigma^2\pi^4\delta^2\delta^{*2} \rightarrow \sigma^2\pi^4\delta^2\delta^{*1}$),¹¹ but in the present system the application of an M_2L_8 bonding scheme is an oversimplification. The combined affect of structural changes and π -delocalization on the extent of Re–Re bonding must be taken into consideration. It is also reasonable to argue that an axial chloride interaction would serve to weaken the σ -component of the metal–metal bond, thus contributing to an overall lengthening of the Re–Re distance.^{11b}

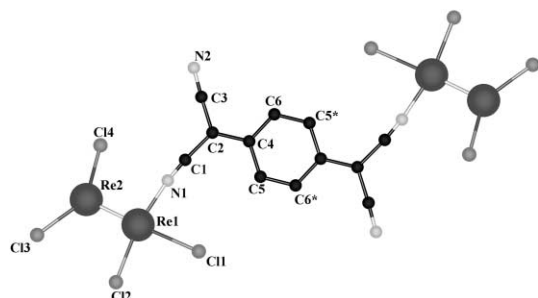


Fig. 5 Crystal Maker representation without dppm ligands of $[\text{Re}_2\text{Cl}_4(\text{dppm})_2]_2(\mu\text{-TCNQ})\cdot 10\text{THF}$.

Other M_2L_9 complexes, such as $\text{Re}_2\text{Cl}_4(\text{dppm})_2(\text{CO})$,¹² have been noted in earlier studies, but these possess A-frame structures, whereas the structural type found in $1\cdot 10\text{THF}$, in which the geometry is trigonal bipyramidal around one of the Re atoms and octahedral around the other Re atom, has been noted only in nitrile complexes of the type $[\text{Re}_2\text{Cl}_3(\text{dppm})_2]$

Table 2 Selected bond distances (Å) and angles (°) for $1\cdot 10\text{THF}$

Re(1)–Re(2)	2.2895(4)	P(1)–C(15)	1.833(7)
Re(1)–Cl(1)	2.5927(17)	P(2)–C(21)	1.837(7)
Re(1)–Cl(2)	2.4024(16)	P(2)–C(27)	1.837(6)
Re(1)–P(1)	2.5066(18)	P(2)–C(7)	1.845(7)
Re(1)–P(3)	2.5080(17)	P(3)–C(39)	1.830(7)
Re(1)–N(1)	2.054(6)	P(3)–C(8)	1.831(7)
Re(2)–Cl(3)	2.3708(17)	P(3)–C(33)	1.840(7)
Re(2)–Cl(4)	2.3709(16)	P(4)–C(8)	1.838(7)
Re(2)–P(2)	2.4542(17)	P(4)–C(45)	1.843(7)
Re(2)–P(4)	2.4440(17)	P(4)–C(51)	1.841(8)
P(1)–C(7)	1.828(6)	N(1)–C(1)	1.023(8)
P(1)–C(9)	1.830(8)	N(2)–C(3)	1.148(10)
N(1)–Re(1)–Re(2)	95.83(14)	Cl(4)–Re(2)–P(4)	84.66(6)
N(1)–Re(1)–Cl(2)	166.07(15)	Cl(3)–Re(2)–P(4)	87.11(6)
Re(2)–Re(1)–Cl(2)	97.71(4)	Re(2)–Re(1)–P(2)	97.34(4)
N(1)–Re(1)–P(1)	97.35(4)	Cl(4)–Re(2)–P(2)	93.60(6)
Cl(2)–Re(1)–P(1)	81.68(6)	Cl(3)–Re(2)–P(2)	83.75(6)
N(1)–Re(1)–P(3)	86.79(15)	P(4)–Re(2)–P(2)	163.39(6)
Cl(2)–Re(1)–P(3)	95.28(6)	C(7)–P(1)–Re(1)	107.1(2)
P(1)–Re(1)–P(3)	167.76(6)	C(9)–P(1)–Re(1)	118.4(2)
N(1)–Re(1)–Cl(1)	81.52(15)	C(15)–P(1)–Re(1)	117.5(2)
Re(2)–Re(1)–Cl(1)	176.41(4)	C(39)–P(3)–Re(1)	117.2(2)
Cl(2)–Re(1)–Cl(1)	85.08(5)	C(8)–P(3)–Re(1)	110.5(2)
P(1)–Re(1)–Cl(1)	85.26(6)	C(21)–P(2)–Re(2)	126.8(2)
P(3)–Re(1)–Cl(1)	82.66(6)	C(27)–P(2)–Re(2)	112.4(2)
Re(1)–Re(2)–Cl(4)	106.60(4)	C(7)–P(2)–Re(2)	103.9(2)
Re(1)–Re(2)–Cl(3)	112.87(5)	C(8)–P(4)–Re(2)	104.5(2)
Cl(4)–Re(2)–Cl(3)	140.47(6)	C(51)–P(4)–Re(2)	111.5(2)
Re(1)–Re(2)–P(4)	98.99(4)	C(45)–P(4)–Re(2)	124.6(2)

(NCR)₂X (X = Cl[−], PF₆[−]) (R = Me, Et, Ph, 4-PhC₆H₄, 1,2-C₆H₄CN) reported by Walton and co-workers.¹³ These complexes contain equatorially bound nitriles and chlorides, and one axially coordinated chloride ligand. Comparisons of the Re–Re, Re–N, and Re–Cl axial distances, and the P–Re–Re–P torsion angles for this structural type are provided in Table 3. The values observed for $1\cdot 10\text{THF}$ are quite similar to those of the $[\text{Re}_2\text{Cl}_3(\text{dppm})_2(\text{NCR})_2]^+$ complexes. The most notable difference appears in the torsion angles, *i.e.*, the P–Re–Re–P twist angle (15.7°) is considerably smaller than the corresponding values in the $[\text{Re}_2\text{Cl}_3(\text{dppm})_2(\text{NCR})_2]^+$ complexes. With a smaller P–Re–Re–P torsion angle and a longer Re–Cl axial distance, one might anticipate a shorter Re–Re distance for $1\cdot 10\text{THF}$ than what is found for the $[\text{Re}_2\text{Cl}_3(\text{dppm})_2(\text{NCR})_2]^+$ complexes, but the converse is true. It is interesting to note that in the structure of the mixed-valence Re^{II}Re^{III} complex $\text{Re}_2\text{Cl}_5(\text{dppm})_2$, the Re–Re separation is 2.263(1) and the P–Re–Re–P torsion angle is 3.99°. The torsion angle is lower, as expected, but the Re–Re distance is similar to other Re^{II}Re^{II} complexes listed in Table 3. This example underscores the danger in equating the Re–Re separation with formal bond order or oxidation state.

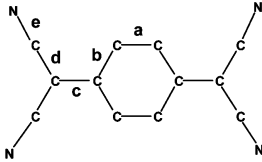
Other pertinent structural features of $1\cdot 10\text{THF}$ are related to the fact that the two rhenium atoms are electronically different which leads to different Re–Cl and Re–P distances. The Re(1)–Cl distances are ~0.04 Å shorter than the Re(2)–Cl_{eq} distance, and the Re(1)–P distances are ~0.07 Å shorter than the Re(2)–P distances. This same trend is also observed in the structure of $\text{Re}_2\text{Cl}_5(\text{dppm})_2$.¹⁴ Once again, these structural differences are attributed to the different coordination environments around each rhenium atom, and assignments of formal charges on either rhenium atom cannot be rationally deduced from these data.

Among the vast reports of TCNQ compounds, there are still relatively few reports of compounds in which TCNQ acts as a ligand. The existence of both terminal σ -TCNQ and σ - μ^4 -TCNQ binding modes for complexes of the unstable $[\text{CpMn}(\text{CO})_2]$ fragment have been proposed on the basis of spectroscopic data, but the formulae have not been verified by crystallography.^{15–17} The crystal structures of various TCNQ^{−1} materials in which the TCNQ behaves as a ligand have been

Table 3 Comparison of selected bond distances (Å) and angles (°) of dirhenium complexes exhibiting an unsymmetrical M_2L_9 geometry

Complex	Re–Re	Re–N	Re–Cl _(axial)	P–Re–Re–P(av.)	Ref
[Re ₂ Cl ₄ (dppm) ₂](μ-TCNQ), 1	2.2895(4)	2.054(6)	2.5927(17)	14.9	This work
[Re ₂ Cl ₃ (dppm) ₂ (NCC ₆ H ₅) ₂][PF ₆]	2.270(1)	2.066(15)	2.575(7)	22.2	13a
[Re ₂ Cl ₃ (dppm) ₂ (NCC ₂ H ₅) ₂][PF ₆]	2.2661(9)	2.01(1)	2.556(4)	30.6	13a
[Re ₂ Cl ₃ (dppm) ₂ (1,2-C ₆ H ₄ (CN) ₂) ₂][PF ₆]	2.265(1)	2.05(3)	2.492(6)	32.4	13a
Re ₂ Cl ₃ (dppm) ₂	2.263(1)		2.575(6)	3.99	14

Table 4 A comparison of bond distances (Å) of several TCNQ containing products

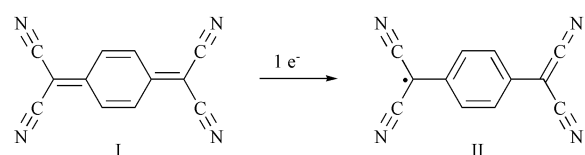
					
Bond	TCNQ	1·10THF	N-MePZT-TCNQ ^a	[Fe(C ₅ Et ₅) ₂][TCNQ] ^b	
a	1.346	1.356	1.349	1.370	
b	1.446, 1.450	1.405, 1.432	1.446	1.418, 1.413	
c	1.374	1.453	1.379	1.423	
d	1.441, 1.440	1.484, 1.440	1.422	1.413, 1.419	
e	1.141, 1.139	1.023, 1.148	1.151	1.148, 1.143	

^a N-Methylphenothiazine-TCNQ, ref. 28a. ^b Ref. 28b.

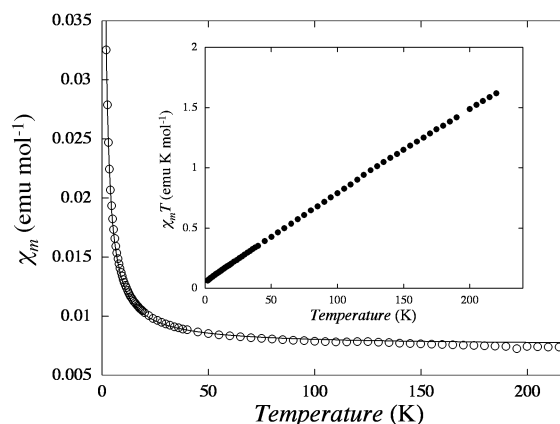
performed by a few research groups, including our own.¹⁸ In our laboratories, we have performed structures on homoleptic metal TCNQ solids of the type $M(\text{TCNQ})$ ($M = \text{Cu}, \text{Ag}$)^{18f} as well as solvated $\text{Mn}(\text{TCNQ})_2 \cdot x\text{S}$ polymers.^{3g} The binding modes vary from *cis*- μ_2 and *syn*- μ_2 to μ_4 -TCNQ in these structures. In the crystal structure of $\text{Ag}(\sigma\text{-}\mu_4\text{-TCNQ})$, the Ag atoms are coordinated to four nitrile positions of independent TCNQ radicals in a distorted tetrahedral arrangement at an average Ag–N distance of 2.322 Å, which is clearly indicative of a M–N interaction.¹⁹ Additionally, a $\sigma\text{-}\mu_4$ -TCNQ ligand has been reported for the complex $[\{\text{Ru}_2(\text{O}_2\text{CCF}_3)_4\}_2(\mu_4\text{-TCNQ}) \cdot 3(\text{C}_7\text{H}_8)]_\infty$ in which one TCNQ is surrounded by four Ru_2 units and creates a 2D hexagonal network.²⁰ In this case, the TCNQ ligand occupies the axial sites of each of the Ru_2 units. The Ru–N_{axial} distance is 2.277(3) Å, which is longer than the Re–N distance in **1**. This is expected since the axial interactions are weaker than equatorial interactions in metal–metal bonded complexes. In the organometallic complex $[(\mu_4\text{-TCNQ})\{\text{fac-Re}(\text{CO})_3(\text{bpy})\}_4]^{4+}$ reported by Kaim *et al.*, the Re–N bond distances are 2.098(7) and 2.121(8).²¹ Both of these values are longer than the Re–N bond distance in **1**, which is reasonable since the TCNQ in the aforementioned complex is neutral, and it is known that the reduced form of TCNQ is a better donor than the neutral form. This further supports our conclusion that charge transfer has occurred between the Re_2 unit and the TCNQ. A perusal of the literature reveals several other various metal–metal complexes that contain $\sigma\text{-TCNQ}$.²²

The bond distances and angles within the TCNQ unit in **1**·10THF are considerably different from those found in structures of TCNQ^0 (Table 4). A comparison of the bond distances in **1**·10THF and other TCNQ^- containing species with those in TCNQ^0 , reveals that bonds *a* and *c* are longer while bonds *b* and *d* are shorter. These bond distances changes are expected and can be explained by a contribution from the resonance structure (**II** in Scheme 1) for TCNQ^- . As reported in the paper by Hoekstra *et al.*, the charges on the reduced forms of TCNQ reside predominately on the N atoms which explains the nucleophilicity of TCNQ^- .^{18b}

(iii) Magnetic properties. The compound $[\text{Re}_2\text{Cl}_4(\text{dppm})_2]_2(\mu\text{-TCNQ}) \cdot 10\text{THF}$, **1**·10THF, is paramagnetic as indicated by the magnetic susceptibility and EPR spectroscopic data. The

**Scheme 1**

χT vs. T plot for **1**·10THF clearly indicates temperature independent paramagnetic (TIP) behavior (Fig. 6). A fitting of $\chi_m = \chi_{\text{TIP}} + C/T$ leads to a value of χ_{TIP} of 7.29×10^{-3} emu mol^{-1} and a paramagnetic “impurity” contribution of $C = 0.0541$ emu K mol^{-1} . The magnitude of the TIP is quite large but this is not unusual based on the fact that Re has a large orbital contribution to its magnetic moment.²³ The EPR spectrum, run at a frequency of 9.52 GHz, of $[\text{Re}_2\text{Cl}_4(\text{dppm})_2]_2(\mu\text{-TCNQ})$, **1**, on a crystalline sample exhibits a broad signal centered at $g = 2.14$ (Fig. 7). The breadth of the signal is indicative of delocalization of spin density onto the Re_2 units, *i.e.*, the system is not that of a localized organic radical.

**Fig. 6** Plot of both the magnetic susceptibility (emu mol^{-1}) and χT (emu K mol^{-1}) vs. temperature (K) of $[\text{Re}_2\text{Cl}_4(\text{dppm})_2]_2(\mu\text{-TCNQ})$.

(iv) Electronic properties. The electronic properties of $[\text{Re}_2\text{Cl}_4(\text{dppm})_2]_2(\mu\text{-TCNQ})$, **1**, are unusual. The parent dirhenium complex $\text{Re}_2\text{Cl}_4(\text{dppm})_2$ exhibits two reversible

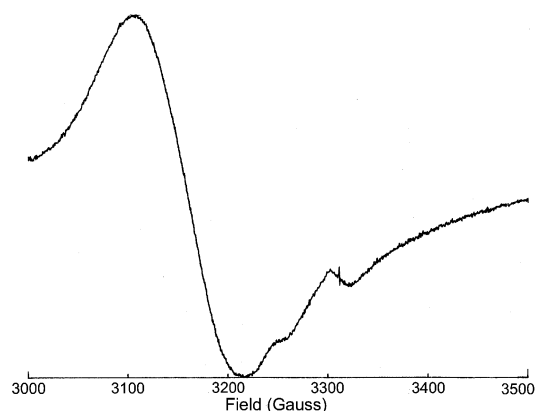


Fig. 7 EPR spectrum of $[\text{Re}_2\text{Cl}_4(\text{dppm})_2]_2(\mu\text{-TCNQ})\cdot 10\text{THF}$ at $-160\text{ }^\circ\text{C}$.

oxidations located at $E_{1/2} = +0.35$ and $+0.87$ V whereas TCNQ exhibits two reversible reductions at $E_{1/2} = +0.28$ and -0.30 V (vs. Ag/AgCl). The cyclic voltammogram (Fig. S1, ESI†) of **1** reveals numerous accessible redox processes, namely one irreversible reduction at $E_{p,c} = -0.19$ V and two reversible oxidations at $E_{1/2} = +0.64$ and $+0.25$ V along with multiple features at potentials greater than $+0.8$ V as observed in the differential pulse voltammogram (Fig. S2, ESI†). These processes are irreversible and occur very close to one another, which renders it difficult to assign precise potentials. From the electronic studies of **1**, it seems reasonable to propose that significant charge transfer has occurred between the dirhenium unit and the TCNQ ligand which leads to delocalization of charge over the entire compound. This delocalization is giving rise to the complex electrochemical properties of **1**.

B. $[\text{Re}_2\text{Cl}_4(\text{dppm})_2]_2(\mu\text{-DM-DCNQI})$, **2**

(i) **Preparation and spectroscopic properties.** The reaction of two equivalents of $\text{Re}_2\text{Cl}_4(\text{dppm})_2$ with DM-DCNQI in THF or benzene leads to microcrystalline samples of $[\text{Re}_2\text{Cl}_4(\text{dppm})_2]_2(\mu\text{-DMDCNQI})$, **2**, directly from the reaction solution. Single crystals were grown using slow diffusion techniques similar to those used to obtain crystals of **1**. The infrared spectrum of **2** exhibits a strong $\nu(\text{C}\equiv\text{N})$ feature at 2056 cm^{-1} , and the electronic absorption spectrum exhibits intense absorptions at $\lambda_{\text{max}} = 1035$ and 1800 nm (Fig. 8). Dichloromethane solutions of **2** are not stable at room temperature as confirmed by the slow decay in intensity of the absorptions in the electronic absorption spectrum.

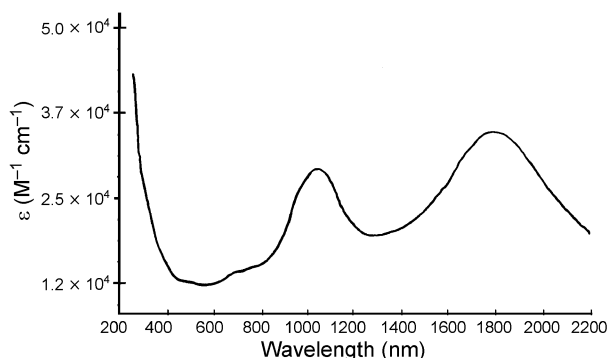


Fig. 8 Electronic absorption spectrum of $[\text{Re}_2\text{Cl}_4(\text{dppm})_2]_2(\mu\text{-DM-DCNQI})$, **2**, in CH_2Cl_2 .

(ii) **X-Ray crystal structure of $[\text{Re}_2\text{Cl}_4(\text{dppm})_2]_2(\mu\text{-DM-DCNQI})\cdot 10\text{THF}$, **2**·10THF.** The molecular structure of **2**·10THF, depicted in Fig. 9, closely resembles the structure of $[\text{Re}_2\text{Cl}_4(\text{dppm})_2]_2(\mu\text{-TCNQ})\cdot 10\text{THF}$ but with the DM-DCNQI moiety

serving to link two $\text{Re}_2\text{Cl}_4(\text{dppm})_2$ molecules through σ -bonds to the two cyano groups. The molecule is centrosymmetric, with the midpoint of the DM-DCNQI moiety being situated on an inversion center. The coordination environments around Re(1) and Re(2) are octahedral and trigonal bipyramidal respectively. The Re–Re distance of $2.2986(5)\text{ \AA}$ is slightly longer than the corresponding distance found in the structure of **1**·10THF ($2.2895(4)\text{ \AA}$). The Re(1)–Cl(1) distance of $2.624(2)\text{ \AA}$ is longer than the other Re–Cl distances, which is not unexpected, given that it occupies an axial site (see Fig. 10). The Re(1)–N(1) distance of $2.033(8)\text{ \AA}$ is slightly shorter than the Re–N distance found in the structure of **1**·10THF ($2.054(6)\text{ \AA}$). Other distances and angles in the dirhenium unit are within the range for derivatives of $\text{Re}_2\text{Cl}_4(\text{dppm})_2$.¹² The three-dimensional structure consists of molecules that stack along the *a*-axis at a distance of $\sim 14\text{ \AA}$ between adjacent DM-DCNQI centers. Closer contacts exist between phenyl rings of the phosphine substituent and among the solvent molecules, but these are not expected to be important pathways for communication between molecules.

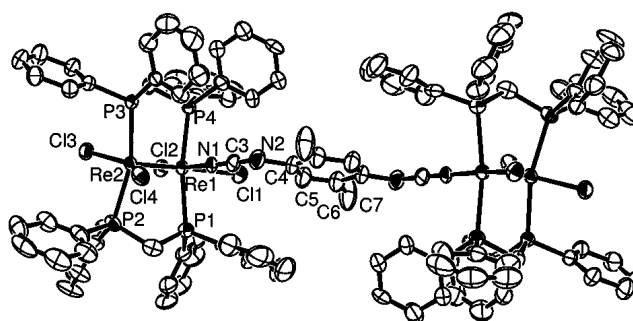


Fig. 9 Thermal ellipsoid representation of $[\text{Re}_2\text{Cl}_4(\text{dppm})_2]_2(\mu\text{-DM-DCNQI})\cdot 10\text{THF}$, **2**·10THF.

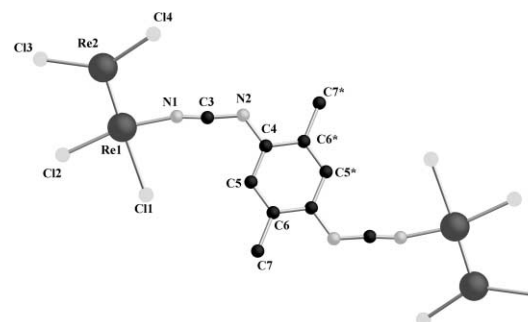


Fig. 10 Crystal Maker representation without the dppm ligands of $[\text{Re}_2\text{Cl}_4(\text{dppm})_2]_2(\mu\text{-DM-DCNQI})\cdot 10\text{THF}$.

(iii) **Magnetic and electronic properties.** As in the case of $[\text{Re}_2\text{Cl}_4(\text{dppm})_2]_2(\mu\text{-TCNQ})$, the molecule $[\text{Re}_2\text{Cl}_4(\text{dppm})_2]_2(\mu\text{-DM-DCNQI})$ is paramagnetic as determined by magnetic susceptibility (Fig. 11) and EPR (signal centered at $g = 2.50$, Fig. 12) measurements. The plot of $\chi_{\text{m}}T$ vs. T (Fig. 11) is typical of temperature independent paramagnetism and is nearly identical to that of compound **1**. An application of the same fitting used for **1** leads to a χ_{TIP} value of $6.23 \times 10^{-3}\text{ emu mol}^{-1}$ and a paramagnetic contribution of $C = 0.108\text{ emu K mol}^{-1}$ for **2**. The electronic properties of **2** are similar to those of **1** (see Fig. S3, ESI†). There are three major redox processes, viz., an irreversible reduction at $E_{p,c} = -0.35$ V and two reversible oxidations at $E_{1/2} = +0.22$ and $+0.69$ V (vs. Ag/AgCl). As was observed for **1**, there are several overlapping irreversible oxidation features. As concluded earlier, such rich electrochemistry is indicative of communication between the redox units through the TCNQ ligand, but a quantitative analysis of the degree of coupling is precluded by the complexity of the voltammograms.

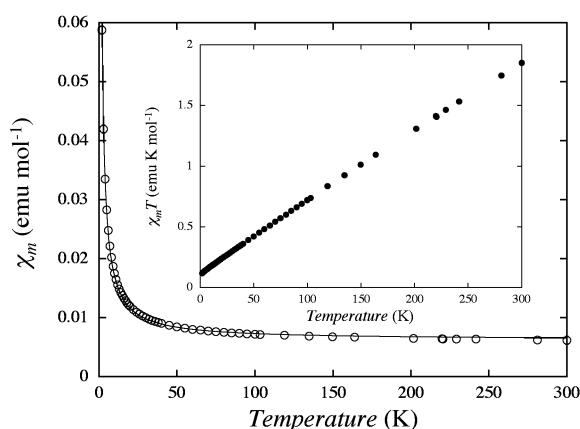


Fig. 11 Plot of both the magnetic susceptibility (emu mol^{-1}) and χT (emu K mol^{-1}) vs. temperature (K) of $[\text{Re}_2\text{Cl}_4(\text{dppm})_2]_2(\mu\text{-DM-DCNQI})$.

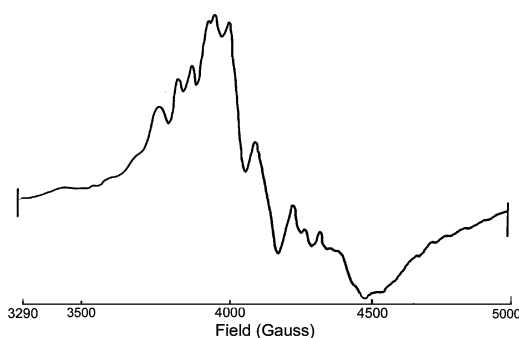


Fig. 12 Solid-state EPR spectrum of $[\text{Re}_2\text{Cl}_4(\text{dppm})_2]_2(\mu\text{-DM-DCNQI})$ 2 at -160°C .

Conclusions

Reactions of two nitrile containing organic acceptors with $\text{Re}_2\text{Cl}_4(\text{dppm})_2$ resulted in the isolation of discrete “dimer-of-dimers” molecules. These compounds which are of the type $[\text{Re}_2\text{Cl}_4(\text{dppm})_2]_2(\mu\text{-L})$, where $\text{L} = \text{TCNQ}$ or DM-TCNQI , exhibit unusual electronic properties and magnetic behavior. The large shift in the $\nu(\text{C}\equiv\text{N})$ bands in the infrared spectra and intense charge-transfer bands in the electronic spectra indicate that interactions between the π -HOMOs of $\text{Re}_2\text{Cl}_4(\text{dppm})_2$ and the π^* orbitals of the TCNQ^{-1} radical are occurring that lead to communication through this network of π orbitals. The intensities of the electronic transitions are remarkably high at $\epsilon \sim 10^4$, which is an indication of mixing of the d-orbitals with the p-orbitals on the ligand that leads to delocalization in the molecule. Attempts to characterize corresponding polymeric structures based on this type of alternating donor/acceptor building blocks are in progress.

Experimental section

Materials

The TCNQ starting material was purchased from TCI and sublimed prior to use. The DM-DCNQI ligand was synthesized according to literature procedures.²⁴ The compound $\text{Re}_2\text{Cl}_4(\text{dppm})_2$ was prepared by an adaptation of the literature procedure.²⁵ In a typical reaction, 25 mL of reagent grade methanol was added to a flask containing $\text{Re}_2\text{Cl}_6(\text{PBU}^n)_2$ ²⁶ (0.750 g, 0.758 mmol) and dppm (1.55 g, 4.03 mmol). The mixture was refluxed for 3 h to yield a purple solid. After the solid had settled out of solution, the supernatant was carefully decanted and the solid was washed with fresh methanol (2×10 mL) followed by diethyl ether. Yield after vacuum drying was 0.88 g (90%).

Physical measurements

IR spectra were recorded as Nujol mulls on KBr plates with the use of a Perkin-Elmer 599 or Perkin-Elmer 1800 FTIR spectrometers. Electronic absorption spectra were measured with Hitachi U-2000 or IBM 9420 UV-visible spectrophotometers, the latter capable of Near IR measurements. The $^{31}\text{P}\{^1\text{H}\}$ spectra were obtained with the use of a Varian XL-200A spectrometer operated at 80.98 MHz or a Varian 300 instrument operated at 121.5 MHz. Electrochemical measurements were carried out on dichloromethane solutions that contained 0.1 M tetra-*n*-butylammonium hexafluorophosphate or tetra-*n*-butylammonium tetrafluoroborate as the supporting electrolyte. Voltammetric experiments were performed with a CH Instruments Electrochemical workstation using a Pt disk as the working electrode. All $E_{1/2}$ values were referenced to the silver/silver chloride (Ag/AgCl) electrode at room temperature. Under our experimental conditions the ferrocenium/ferrocene couple occurs at $E_{1/2} = +0.47$ V vs. Ag/AgCl . Variable-temperature magnetic susceptibility measurements were carried out on solid microcrystalline samples on a Quantum Design MPMS-2 SQUID magnetometer in the range of 2–300 K.

Preparation of $[\text{Re}_2\text{Cl}_4(\text{dppm})_2]_2(\mu\text{-TCNQ})$, 1

(i) Bulk reaction. A solution containing TCNQ (0.0120 g, 0.059 mmol) in THF (15 mL) was added to a 15 mL THF solution containing $\text{Re}_2\text{Cl}_4(\text{dppm})_2$ (0.150 g, 0.117 mmol). The mixture was stirred for several minutes and left to stand undisturbed overnight at r. t. to yield a crop of black microcrystals. The product was collected by filtration, washed with THF (3×5 mL), and dried *in vacuo*; yield 0.140 g (86%). Anal. Calc. for $\text{C}_{120}\text{H}_{108}\text{N}_4\text{Cl}_8\text{O}_2\text{P}_8\text{Re}_4$: C, 49.45; H, 3.74; Cl, 9.73. Found: C, 49.38; H, 3.48; Cl, 9.62%. IR (CsI, Nujol, cm^{-1}): $\nu(\text{C}\equiv\text{N})$ 2187 (m), 2109 (s, br), $\nu(\text{C}=\text{C})$ 1573 (m), 1586 (w, sh). $^{31}\text{P}\{^1\text{H}\}$ NMR (CDCl_3): δ –14 ppm. Electronic spectroscopy (CH_2Cl_2): $\lambda_{\text{max}}/\text{nm}$ ($\epsilon/\text{M}^{-1}\text{cm}^{-1}$), 1080 (2.56×10^4), 1980 (2.20×10^4).

(ii) Slow diffusion reaction. Separate stock solutions of $\text{Re}_2\text{Cl}_4(\text{dppm})_2$ (0.150 g, 0.117 mmol, 15 mL of THF) and TCNQ (0.0120 g, 0.059 mmol, 15 mL of THF) were prepared. A 2 mL quantity of the $\text{Re}_2\text{Cl}_4(\text{dppm})_2$ solution was syringed into an 8 mm O.D. Pyrex tube and carefully layered with 2 mL of THF followed by 2 mL of the TCNQ stock solution. The tubes were flame sealed under vacuum. After ten days, a crop of black crystals had formed at the interface of the layers in each tube (7 tubes total); these were harvested and washed with THF; combined yield 10 mg (6%). IR (CsI, Nujol, cm^{-1}): $\nu(\text{C}\equiv\text{N})$ 2186 (m), 2104 (s, br), $\nu(\text{C}=\text{C})$ 1572 (m), 1586 (w, sh).

Preparation of $[\text{Re}_2\text{Cl}_4(\text{dppm})_2]_2(\mu\text{-DM-DCNQI})$, 2

(i) Bulk reaction. A solution containing 0.0073 g (0.039 mmol) of DM-DCNQI in 20 mL of benzene was slowly added to a stirring solution containing 0.100 g (0.078 mmol) of $\text{Re}_2\text{Cl}_4(\text{dppm})_2$ in 10 mL of benzene. Initially the solution turned dark blue, and after 10 min a black solid was collected by filtration, washed with benzene and vacuum dried; yield 0.084 g (78%). IR (CsI, Nujol, cm^{-1}): $\nu(\text{C}\equiv\text{N})$ 2056 (s,br), $\nu(\text{C}=\text{C})$ 1586 (w). Anal. Calc. for $\text{C}_{110}\text{H}_{96}\text{N}_4\text{Cl}_8\text{P}_8\text{Re}_4$: C, 48.04; H, 3.52; N, 2.04. Found C, 47.98; H, 3.81; N, 2.01%. A $^{31}\text{P}\{^1\text{H}\}$ NMR signal was not observed. Electronic spectroscopy (CH_2Cl_2): $\lambda_{\text{max}}/\text{nm}$ ($\epsilon/\text{M}^{-1}\text{cm}^{-1}$), 696 (sh), 1035 (2.7×10^4), 1800 (3.6×10^4).

Similar results were obtained when THF was used as the reaction solvent.

(ii) Slow diffusion reaction. A quantity of DM-DCNQI (0.0073 g, 0.039 mmol) was dissolved in 5 mL of THF and slowly added to a Schlenk tube containing 0.100 g (0.078 mmol)

Table 5 Crystallographic information for both compounds **1**·10THF and **2**·10THF

	1 ·10THF	2 ·10THF
Formula	C ₁₅₂ H ₁₇₂ Cl ₈ N ₄ O ₁₀ P ₈ Re ₄	C ₁₅₀ H ₁₇₆ Cl ₈ N ₄ O ₁₀ P ₈ Re ₄
<i>M_w</i>	3491.10	3445.25
Space group	<i>P</i> $\bar{1}$	<i>P</i> $\bar{1}$
<i>T</i> /K	173(2)	173(2)
$\lambda/\text{\AA}$	0.71073	0.71073
<i>a</i> /\AA	12.1888(3)	12.2278(2)
<i>b</i> /\AA	14.2908(3)	14.3701(2)
<i>c</i> /\AA	23.3215(6)	23.2604(3)
α°	72.8220(10)	74.6360(10)
β°	81.9380(10)	83.2270(10)
γ°	75.7760(10)	75.4460(10)
<i>V</i> /\AA ³	3752.06(16)	3808.88
<i>Z</i>	1	1
<i>D_c</i> /g cm ^{−3}	1.545	1.513
$\mu(\text{Mo-K}\alpha)/\text{mm}^{-1}$	3.501	3.448
<i>R</i> (<i>I</i> > 2.00σ(<i>I</i>))	0.0430	0.0571
<i>R</i> (all data)	0.0670	0.0920
<i>R_w</i> (<i>I</i> > 2.00σ(<i>I</i>))	0.0972	0.1353
<i>R_w</i> (all data)	0.1062	0.1478 (all data)

of Re₂Cl₄(dppm)₂ dissolved in 5 mL of THF. The Schlenk tube was placed in the refrigerator for 2 days after which time black crystals were observed to have formed; these were collected by filtration, washed with THF, and dried *in vacuo*; yield 0.076 g (71%).

X-Ray data collection, reduction, and structure determination

Single crystals for the crystallographic analyses were mounted on glass fibers and secured with Dow-Corning grease. The crystal dimensions are 0.39 × 0.26 × 0.09 mm³ for **1** and 0.50 × 0.35 × 0.20 mm³ for **2**. Data were collected on a Siemens SMART 1K CCD platform diffractometer in the range of 1.53 < 2θ < 24.71° for **1** and 1.51 < 2θ < 24.71° for **2** at 173(2) K with graphite-monochromated Mo-Kα radiation (λ = 0.71073 Å). Of the total 23479 reflections for **1** and 24165 reflections for **2** that were collected, 12635 and 12830 are unique, respectively. The structures were solved by direct methods (SHELXTL v5.04)^{27a} and refined by full-matrix least-squares calculations on *F*² (SHELXL-97).^{27b} The non-hydrogen atoms were refined anisotropically, whereas hydrogen atoms were calculated and fixed during refinement. Full-matrix least-squares refinement based on 9396 observed reflections for **1** and 8559 observed reflections for **2** (*I* > 2.00σ(*I*)) were employed. The unweighted and weighted agreement factors of *R* = Σ||*F_o*| − |*F_c*||/Σ|*F_o*| and *R_w* = [Σw(|*F_o*| − |*F_c*|)²/Σw|*F_o*|²]^{1/2} were used. The crystal data and details of the structure determination are summarized in Table 5.

CCDC reference numbers 209028 and 209029.

See <http://www.rsc.org/suppdata/dt/b3/b304509a/> for crystallographic data in CIF or other electronic format.

Acknowledgements

K. R. D. gratefully acknowledges the National Science Foundation for a PI Grant (CHE-9906583) and for equipment grants to purchase the CCD X-ray equipment (CHE-9807975) and the SQUID magnetometer (NSF-9974899). We also wish to thank both Texas A&M University and Michigan State University for additional financial support.

References

- (a) J. R. Ferraro and J. M. Williams, *Introduction to Synthetic Electrical Conductors*, Academic Press, Inc., New York, 1987; (b) J. M. Williams, A. J. Schultz, U. Geiser, K. D. Carlson, A. M. Kini, H. H. Wang, W.-K. Kwok, M.-H. Whangbo and J. E. Schirber, *Science*, 1991, **252**, 1501; (c) M. R. Bryce, *Chem. Soc. Rev.*, 1991, **20**, 355; (d) Proceedings of the International Conference on Science and Technology of Synthetic Metals (ICSM88) Santa Fe, NM, USA, *Synth. Met.*, 1988, B1–B656.
- See, for example: (a) C. Kollmar and O. Kahn, *Acc. Chem. Res.*, 1993, **26**, 259; (b) R. M. White, *Science*, 1985, **229**, 11; (c) O. Kahn, *Molecular Magnetism*, VCH, New York, 1993; (d) J. S. Miller, *Adv. Mater.*, 1992, **4**, 298; (e) H. O. Stumpf, Y. Pei, C. Michaut, O. Kahn, J. R. Renard and L. Ouahab, *Chem. Mater.*, 1994, **6**, 257; (f) P. Rey, *Acc. Chem. Res.*, 1989, **22**, 392; (g) A. Caneschi, D. Gatteschi, J. P. Renard, P. Rey and R. Sessoli, *Inorg. Chem.*, 1989, **28**, 3314; (h) J. R. Galán-Mascarós, C. Giménez-Saiz, S. Triki, C. J. Gómez-García, E. Coronado and L. Ouahab, *Angew. Chem., Int. Ed. Engl.*, 1995, **34**, 1460.
- (a) J. Zhang, J. Ensling, V. Ksenofontov, P. Gülich, A. J. Epstein and J. S. Miller, *Angew. Chem., Int. Ed. Engl.*, 1998, **37**, 657; (b) J. S. Miller and A. J. Epstein, *Angew. Chem. Int. Ed.*, 1994, **33**, 385; (c) J. S. Miller, A. J. Epstein and W. M. Reiff, *Chem. Rev.*, 1988, **88**, 201; (d) J. S. Miller, J. C. Calabrese, H. Rommelmann, S. R. Chittipeddi, H. H. Zhang, W. M. Reiff and A. J. Epstein, *J. Am. Chem. Soc.*, 1987, **109**, 769; (e) M. S. Ward and D. C. Johnson, *Inorg. Chem.*, 1987, **26**, 4213; (f) W. E. Broderick, J. A. Thompson, E. P. Day and B. M. Hoffman, *Science*, 1990, **249**, 401; (g) H. Zhao, R. A. Heintz, X. Ouyang, K. R. Dunbar, C. F. Campana and R. D. Rogers, *Chem. Mater.*, 1999, **11**, 736; (h) R. Clérac, S. O'Kane, J. Cowen, X. Ouyang, R. Heintz, H. Zhao, M. J. Bazile, Jr. and K. R. Dunbar, *Chem. Mater.*, 2003, **15**, 1840.
- J. M. Manriquez, G. T. Yee, R. S. McLean, A. J. Epstein and J. S. Miller, *Science*, 1991, **252**, 1415.
- (a) T. C. Zietlow, D. D. Klendworth, T. Nimry, D. J. Salmon and R. A. Walton, *Inorg. Chem.*, 1981, **20**, 947; (b) T. J. Barder, F. A. Cotton, D. Lewis, W. Schwotzer, S. M. Tetrick and R. A. Walton, *J. Am. Chem. Soc.*, 1984, **106**, 2882.
- Scan rate 200 mV s^{−1}, 0.1 M TBAH, in CH₂Cl₂. The Cp₂Fe⁰/Cp₂Fe⁺ couple was referenced at +0.47 V.
- H. Taube and A. Johnson, *J. Indian Chem. Soc.*, 1989, **66**, 503.
- (a) B. Lunelli and C. Pecile, *J. Chem. Phys.*, 1979, **52**, 2375; (b) W. Pukacki, M. Pawlak, A. Graja, M. Lequan and R. M. Lequan, *Inorg. Chem.*, 1987, **26**, 1328; (c) W. Kaim and M. Moscherosh, *Coord. Chem. Rev.*, 1994, **129**, 157; (d) J. G. Robles-Martínez, A. Salmeron-Valverde, E. Alonso and C. Soriano, *Inorg. Chem. Acta*, 1991, **179**, 149.
- S. L. Bartley and K. R. Dunbar, *Angew. Chem., Int. Ed.*, 1991, **30**, 448.
- (a) P. E. Fanwick, A. C. Price and R. A. Walton, *Inorg. Chem.*, 1988, **27**, 2601; (b) A. C. Price and R. A. Walton, *Polyhedron*, 1987, **6**, 729.
- (a) For a study on the effect of bond length on bond order of M₂L₈ complexes, see: F. A. Cotton, K. R. Dunbar, L. R. Falvello, M. Tomas and R. A. Walton, *J. Am. Chem. Soc.*, 1983, **105**, 4950; (b) for a description the elongation of metal–metal bonds due to axial ligation, see: F. A. Cotton and R. A. Walton, in *Multiple Bonds between Metal Atoms*, Clarendon Press, Oxford, 2nd edn., 1987, ch. 2.
- F. A. Cotton, K. R. Dunbar, A. C. Price, W. Schwotzer and R. A. Walton, *J. Am. Chem. Soc.*, 1986, **108**, 4843.
- (a) T. J. Barder, F. A. Cotton, L. R. Falvello and R. A. Walton, *Inorg. Chem.*, 1985, **24**, 1258; (b) D. R. Derringer, K.-Y. Shih, P. E. Fanwick and R. A. Walton, *Polyhedron*, 1991, **10**, 79; (c) P. E. Fanwick, J.-S. Qi, K.-Y. Shih and R. A. Walton, *Inorg. Chim. Acta*, 1990, **172**, 65.
- F. A. Cotton, L. W. Shive and B. R. Stults, *Inorg. Chem.*, 1976, **15**, 2239.
- R. Gross and W. Kaim, *Angew. Chem., Int. Ed.*, 1987, **26**, 251.
- B. Olbrich-Deussner, R. Gross and W. Kaim, *J. Organomet. Chem.*, 1989, **366**, 155.
- R. Gross-Lannert, W. Kaim and B. Olbrich-Deussner, *Inorg. Chem.*, 1990, **29**, 5046.
- (a) C. J. Fritchie and P. Arthur, *Acta Crystallogr.*, 1966, **21**, 139; (b) A. Hoekstra, T. Spoelder and A. Vos, *Acta Crystallogr., Sect. B*, 1972, **28**, 14; (c) M. Konno and Y. Saito, *Acta Crystallogr., Sect. B*, 1974, **30**, 1294; (d) S. A. O'Kane, R. Clérac, H. Zhao, X. Ouyang, J. R. Galán-Mascarós, R. Heintz and K. R. Dunbar, *J. Solid State Chem.*, 2000, **152**, 159; (e) C. Campana, K. R. Dunbar and X. Ouyang, *Chem. Commun.*, 1996, 2427; (f) R. A. Heintz, H. Zhao, X. Ouyang, G. Grandinetti, J. Cowen and K. R. Dunbar, *Inorg. Chem.*, 1999, **38**, 144; (g) H. Zhao, M. J. Bazile, Jr, J. R. Galán-Mascarós and K. R. Dunbar, *Angew. Chem., Int. Ed.*, 2003, **42**, 1015.
- L. Shields, *J. Chem. Soc., Faraday Trans. 2*, 1985, **81**, 1.
- H. Miyasaka, C. S. Campos-Fernández, R. Clérac and K. R. Dunbar, *Angew. Chem., Int. Ed.*, 2000, **39**, 3831.

- 21 H. Hartmann, W. Kaim, I. Hartenbach, T. Schleid, M. Wanner and J. Fiedler, *Angew. Chem., Int. Ed.*, 2001, **40**, 2842.
- 22 (a) H. Miyasaka, C. S. Campos-Fernández, R. Clérac and K. R. Dunbar, *Angew. Chem., Int. Ed.*, 2000, **39**, 3831; (b) C. Campana, K. R. Dunbar and X. Ouyang, *Chem. Commun.*, 1996, 2427; (c) W. Kaim and M. Moscherosh, *Coord. Chem. Rev.*, 1994, **129**, 157; (d) L. Ballester, A. Gutiérrez, M. F. Perpiñán and M. T. Azcondo, *Coord. Chem. Rev.*, 1999, **190**, 447.
- 23 (a) K. R. Dunbar, E. J. Schelter, B. S. Tsukerbalt, S. M. Ostrovsky, V. Y. Mirovitsky and A. V. Pali, *Polyhedron*, 2003, in press; (b) K. R. Dunbar, E. J. Schelter, B. S. Tsukerblat, A. V. Pali, S. M. Ostrovsky, V. Y. Mirovitsky and A. V. Pali, *Adv. Quantum Chem.*, 2003, in press; (c) K. R. Dunbar, E. J. Schelter, B. S. Tsukerblat, S. M. Ostrovsky, V. Y. Mirovitsky and A. V. Pali, *J. Chem. Phys. A*, submitted.
- 24 A. Aumüller and S. Hünig, *Liebigs Ann. Chem.*, 1986, 142.
- 25 T. J. Barder, F. A. Cotton, K. R. Dunbar, G. L. Powell, W. Schwotzer and R. A. Walton, *Inorg. Chem.*, 1985, **24**, 2550.
- 26 J. San Filippo, Jr., *Inorg. Chem.*, 1972, **11**, 3140.
- 27 (a) G. M. Sheldrick, SHELXTL Crystallographic Software Package, Version 5.04, Bruker-AXS, Wisc. 1997; (b) G. M. Sheldrick, SHELXL-97, Program for Refinement of Crystal Structure, University of Göttingen, Göttingen, Germany, 1997.
- 28 (a) H. Kobayahi, *Bull. Chem. Soc. Jpn.*, 1973, **46**, 2945; (b) K. Chi, J. C. Calabrese, W. M. Reiff and J. S. Miller, *Organometallics*, 1991, **10**, 688.